The Plant Cell, Vol. 1, 1011–1023, October 1989 © 1989 American Society of Plant Physiologists

Changes in the Zein Composition of Protein Bodies during Maize Endosperm Development

Craig R. Lending[a] and Brian A. Larkins[b,1]

[a] Department of Botany and Plant Pathology, Purdue University, West Lafayette, Indiana 47907
[b] Department of Plant Sciences, University of Arizona, Tucson, Arizona 85721

Zeins, the seed storage proteins of maize, are synthesized during endosperm development by membrane-bound polyribosomes and transported into the lumen of the endoplasmic reticulum, where they assemble into protein bodies. To better understand the distribution of the various zeins throughout the endosperm, and within protein bodies, we used immunolocalization techniques with light and electron microscopy to study endosperm tissue at 14 days and 18 days after pollination. Protein bodies increase in size with distance from the aleurone layer of the developing endosperm; this reflects a process of cell maturation. The protein bodies within the subaleurone cell layer are the smallest and contain little or no α-zein; β-zein and γ-zein are distributed throughout these small protein bodies. The protein bodies in cells farther away from the aleurone layer are progressively larger, and immunostaining for α-zein occurs over locules in the central region of these protein bodies. In the interior of the largest protein bodies, the locules of α-zein are fused. Concomitant with the appearance of α-zein in the central regions of the protein bodies, most of the β- and γ-zeins become peripheral. These observations are consistent with a model in which specific zeins interact to assemble the storage proteins into a protein body.

INTRODUCTION

The endosperm of developing maize seeds contains a group of alcohol-soluble storage proteins called zeins. These proteins are synthesized 10 days to 40 days after pollination (DAP) and constitute approximately 50% of the total protein in the mature seed (Lee et al., 1976). Zeins are synthesized by membrane-bound polyribosomes and transported into the lumen of the endoplasmic reticulum, where they assemble into protein bodies (Khoo and Wolf, 1970; Larkins and Hurkman, 1978).

Zeins are classified according to their solubility in alcoholic solutions in the presence or absence of reducing agents, such as β-mercaptoethanol (Landry and Moureaux, 1970; Wallace et al., 1989). Total zein can be resolved into polypeptides with apparent molecular mass of 27 kD, 22 kD, 19 kD, 16 kD, 14 kD, and 10 kD by SDS-PAGE (Larkins et al., 1984). Esen (1986) divided the proteins into classes designated α-, β-, and γ-zeins that correspond to the M_r 22,000 and 19,000, the M_r 16,000 and 14,000, and the M_r 27,000 components, respectively. However, the M_r 16,000 protein is structurally more similar to the M_r 27,000 protein than to the M_r 14,000 protein (Prat, Pérez-Grau, and Puigdomènech, 1987), and should probably be considered a γ-zein. The M_r 10,000 protein is structurally different from the others (Kirihara et al., 1988) and constitutes a fourth class, δ-zein (Wallace et al., 1989).

[1] To whom correspondence should be addressed.

The distribution of protein bodies in developing maize kernels has been examined by light microscopy (Kiesselbach, 1949; Wolf, Khoo, and Seckinger, 1969) and electron microscopy (Khoo and Wolf, 1970; Larkins and Hurkman, 1978). Additionally, protein bodies have been examined in studies of the aleurone layer (Kyle and Styles, 1977), the embryo (Schel, Kieft, and VanLammeren, 1984), and endosperm suspension cultures (Felker, 1987). These studies were all performed with routine histochemical staining procedures, which could not distinguish among the different classes of zeins. An attempt to employ fluorescent-labeled antibodies to localize zeins with the light microscope was equivocal (Dierks-Ventling and Ventling, 1982).

Immunolocalization techniques with isolated protein bodies have recently shown that the different classes of zeins are distributed heterogeneously within these organelles. Ludevid et al. (1984) demonstrated that γ-zein is located at the periphery of isolated protein bodies. We also observed that γ-zein is generally located in the peripheral region of isolated protein bodies; the immunostaining patterns corresponded to dark-staining regions of protein bodies that were post-stained with uranyl acetate and lead citrate (Lending et al., 1988). Additionally, we found that β-zein had a staining pattern similar to that of γ-zein, although the intensity of the immunostaining was generally greater for β-zein than for γ-zein. Although most of the immunostaining occurred in the peripheral regions of pro-

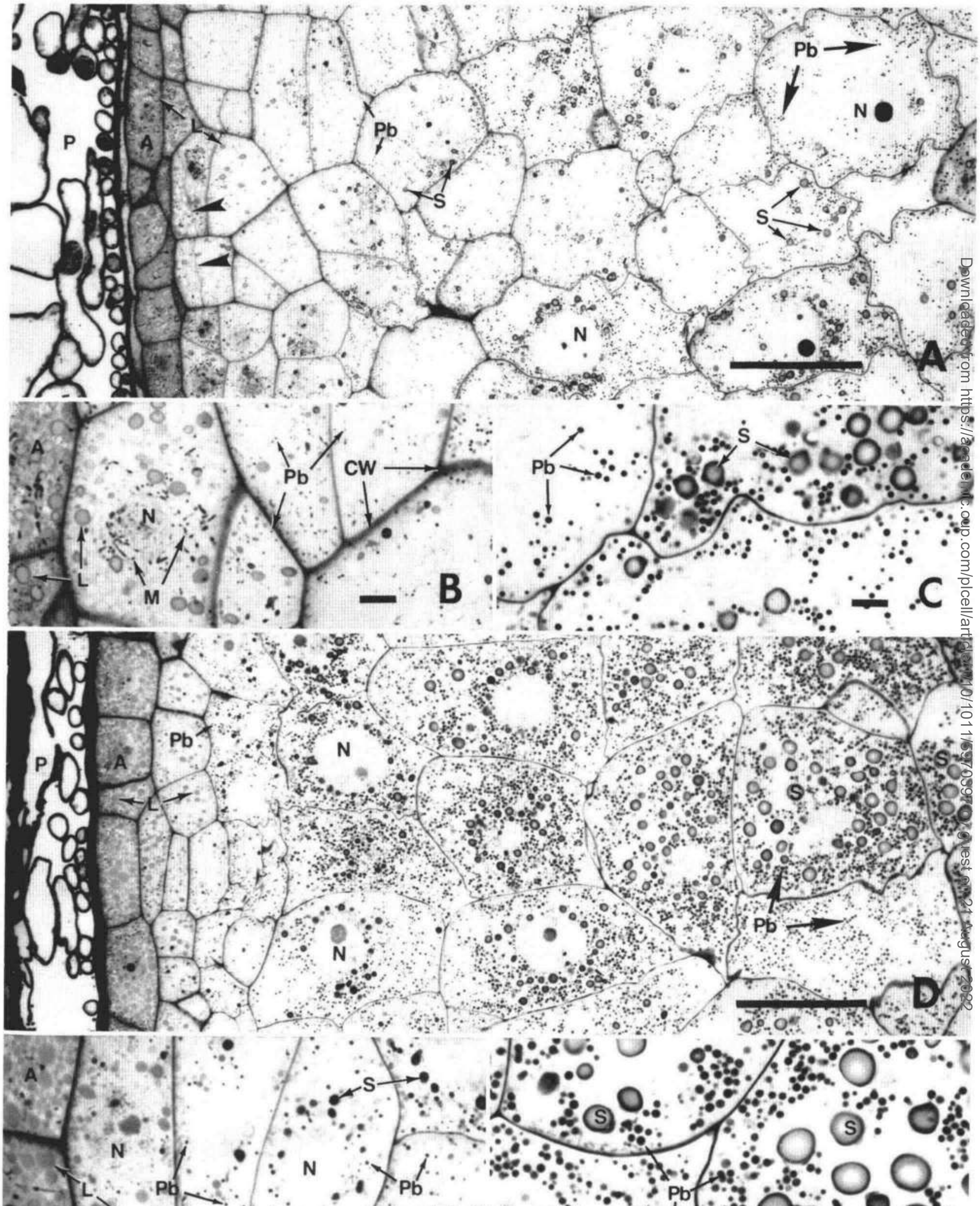

tein bodies, some internal deposits of dark-staining material stained strongly for β-zein and/or γ-zein. α-Zein was generally located in the internal regions of protein bodies or within discrete locules; this immunostaining corresponded to light-staining regions of the protein bodies that were post-stained with uranyl acetate and lead citrate.

In addition to the heterogeneous distribution of the α-, β-, and γ-zeins within individual protein bodies, there was considerable variation in the size of isolated protein bodies (Lending et al., 1988). The protein bodies isolated from the inbred line W64A at 18 DAP were nearly spherical, with diameters ranging from 0.3 μm to 1.3 μm, although the majority were between 0.8 μm and 1.2 μm.

The present study was undertaken to determine the distribution of protein bodies of different sizes and morphologies in maize endosperm. We used immunocytochemical techniques at the light and electron microscopic levels to determine both the distribution of the various zeins within protein bodies and the distribution of the various types of protein bodies within developing regions of the endosperm. These studies help elucidate the spatial and temporal formation of protein bodies. We propose a model describing the developmental sequence for the formation of protein bodies in developing maize endosperm.

RESULTS

Terminology

We used the convention established by Khoo and Wolf (1970) to describe the cell layers in the endosperm. The cell layer immediately beneath the aleurone is termed the subaleurone. The cells beneath the subaleurone layer are called the starchy endosperm; the first starchy endosperm layer is adjacent to the subaleurone layer, and the numbering of cell layers increases with distance from the subaleurone layer.

Endosperm Structure—Light Microscopy

14 Days after Pollination

Proteins in the cytoplasm of the endosperm stained very lightly with basic fuchsin in tissue sampled 14 DAP, as shown in Figure 1A. The endosperm cells were larger with increasing distance from the aleurone layer, and cell divisions were often observed in the subaleurone layer.

Cells of the subaleurone layer contained few protein bodies (as determined by electron microscopy); the first protein bodies recognizable with the light microscope were located in the first starchy endosperm layer and were approximately 0.25 μm in diameter (Figure 1B). More protein bodies were found toward the interior of the developing endosperm (Figure 1C). The size of protein bodies increased with increasing distance from the aleurone layer, and those in the sixth starchy endosperm layer were approximately 0.6 μm in diameter (Figure 1C). Starch grains were dispersed throughout the larger cells of the endosperm (Figures 1A and 1C), and often surrounded nuclei (Figure 1A). The aleurone layer contained many lipid bodies (Figures 1A and 1B); these were also observed in the subaleurone and the first few starchy endosperm cell layers, although they generally became smaller with increasing distance from the aleurone layer.

18 Days after Pollination

The staining density of the cytoplasm increased between 14 DAP and 18 DAP when tissue was stained with basic fuchsin (compare Figure 1D with Figure 1A). Protein bodies and starch granules were the predominant components in cells of developing endosperm sampled at 18 DAP. Unlike tissue sampled at 14 DAP, few dividing cells were observed in the subaleurone layer.

In contrast to the subaleurone cells at 14 DAP, protein bodies were found in these cells at 18 DAP (Figure 1E);

Figure 1. Photomicrographs of Sections Through Developing Maize Endosperm at 14 DAP and 18 DAP, Stained with Basic Fuchsin.

The abbreviations used are: A, aleurone; CW, cell wall; L, lipid body; M, mitochondrion; N, nucleus; Pb, protein body; S, starch grain.
(A) Low magnification view of endosperm at 14 DAP. The size of protein bodies (Pb, small arrows) gradually increases in cells farther from the aleurone layer (Pb, large arrows). Frequent cell divisions are seen (arrowheads). Bar = 50 μm.
(B) High magnification view of the aleurone, subaleurone, and the first, second, and third starchy endosperm layers at 14 DAP. Some protein bodies are found in the subaleurone layer, although it is not possible to distinguish them from mitochondria at this level of resolution. The number of protein bodies increases in cells farther from the aleurone. Bar = 5 μm.
(C) High magnification view of the sixth and seventh starchy endosperm layers at 14 DAP. Bar = 5 μm.
(D) Low magnification view of endosperm at 18 DAP. The number of protein bodies increases substantially between 14 DAP and 18 DAP [compare **(D)** with **(A)**]. The size of protein bodies (PB, small arrows) gradually increases in cells farther from the aleurone layer (PB, large arrows). Bar = 50 μm.
(E) High magnification view of the aleurone layer, subaleurone, and the first, second, and third starchy endosperm layers at 18 DAP. Protein bodies are visible in the subaleurone layer and all of the interior cells. Bar = 5 μm.
(F) High magnification view of the sixth and seventh starchy endosperm layers at 18 DAP. Protein bodies and starch grains in this region of the endosperm have both increased in size compared with 14 DAP [compare **(F)** with **(C)**]. Bar = 5 μm.

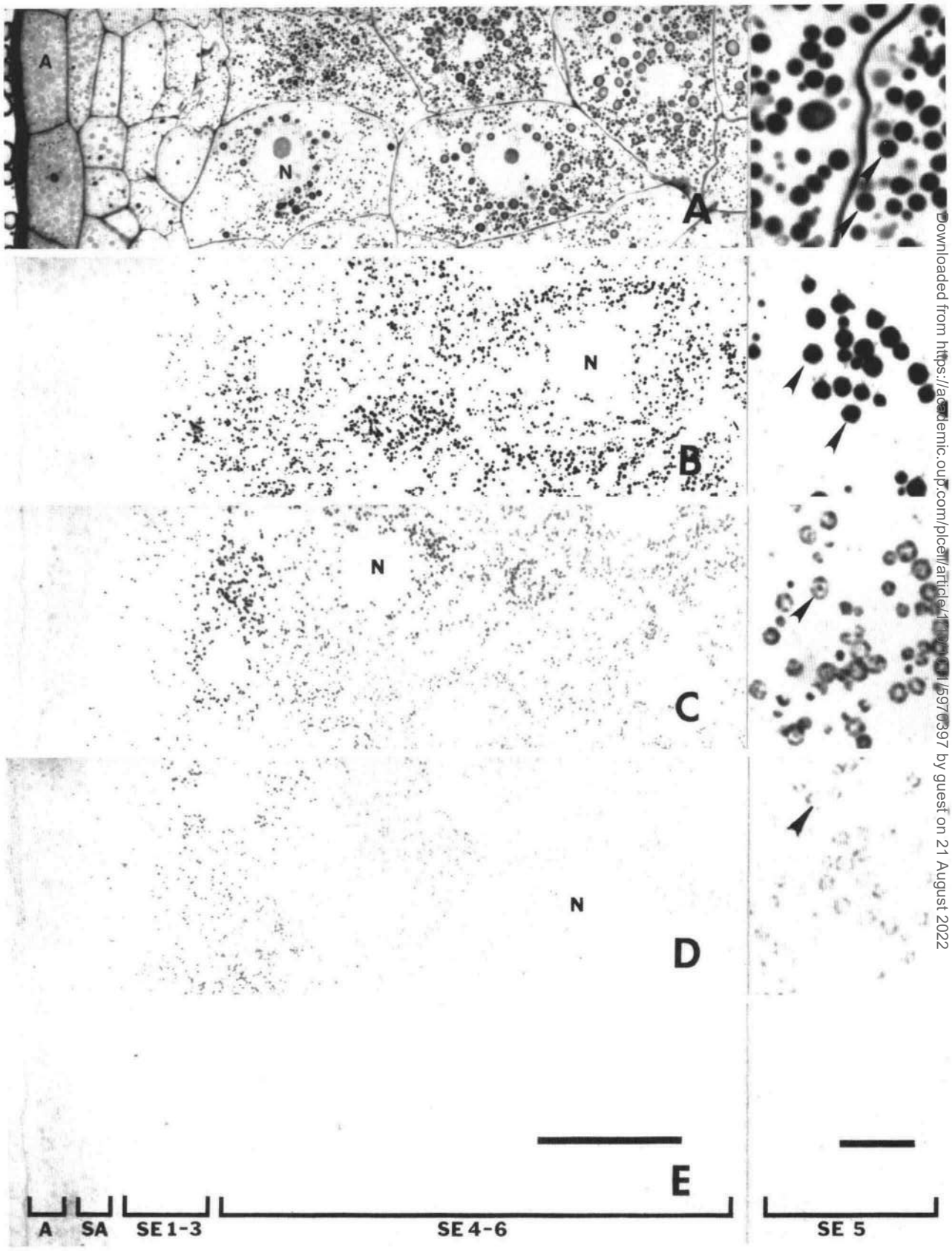

these were approximately 0.25 μm in diameter. The size of the protein bodies gradually increased with distance from the subaleurone layer, and those within the sixth starchy endosperm layer were approximately 1 μm in diameter (Figure 1F). Protein bodies in interior cells of the endosperm were uniformly distributed throughout the cytoplasm; starch grains were generally found in the central regions of the cells (Figure 1F), often encircling nuclei (Figure 1D). The aleurone layer contained many lipid bodies; their number and size decreased in cell layers farther from the aleurone layer (Figures 1D and 1E).

Immunolocalization of Zeins—Light Microscopy

14 Days after Pollination

Because of the low abundance and small size of protein bodies at 14 DAP, immunostaining did not provide much information. Thus, this tissue was studied primarily by electron microscopy.

18 Days after Pollination

Figure 2A shows a semi-thin section of endosperm stained with basic fuchsin; it is similar to the immunostained sections, and is included to compare with regions that are immunostained (Figures 2B to 2E). The designation of the various cell layers is indicated at the bottom of Figure 2.

In sections of endosperm sampled at 18 DAP, light immunolabeling with the α-zein antibody was observed in the subaleurone cell layer and in the first layer of starchy endosperm, although it is not apparent at the magnification shown (Figure 2B). The intensity of staining increased in cell layers deeper in the endosperm, and became more or less constant by the third starchy endosperm layer. The immunostaining formed solid circular deposits; the diameter of the deposits increased from the subaleurone layer inward, and became constant at approximately the third subaleurone layer. The staining patterns were similar in size to that of the underlying protein bodies (Figure 2B, inset).

Immunostaining with the β-zein antibody was visible within the subaleurone layer, unlike that observed for α-zein (Figure 2C). The labeling intensity was greatest in the second through the fourth starchy endosperm layers and was less in cells farther from the aleurone. The immunostaining in the first few cells beneath the aleurone layer formed solid circular patterns (not apparent at the magnification shown). In the cells farther from the aleurone layer, the immunolabeling for β-zein formed open circular patterns of varying intensity; although most of the immunostaining occurred over the peripheral regions of the protein bodies, central inclusions often stained (Figure 2C, inset).

The overall immunostaining pattern with the γ-zein antibody was similar to that for β-zein; labeling was observed in the first few cell layers immediately beneath the aleurone layer (Figure 2D) and decreased at greater distances from the aleurone layer. The immunostaining in the first few cells beneath the aleurone layer formed solid circular patterns, similar to the β-zein immunostaining, although it was not as dense as that observed for β-zein (not apparent at the magnification shown). Although the labeling pattern for γ-zein in the interior cells of the endosperm was similar to

Figure 2. Photomicrographs of Endosperm 18 DAP, Illustrating the Immunostaining Patterns with Antibodies Directed Against α-, β-, and γ-zeins.

Bar = 50 μm, and bar = 5 μm for all insets. Abbreviations are as in Figure 1. Brackets at bottom indicate approximate cell position. A, aleurone; SA, subaleurone; SE, starchy endosperm. See Results (Terminology) for further information on the designation of cell positions.
(A) Sections stained with basic fuchsin illustrating a region similar to those immunostained with the various antibodies. **(Inset)** High magnification view of the fifth starchy endosperm layer. Most protein bodies from this region of the endosperm are from 0.8 μm to 1.4 μm in diameter (arrowheads).
(B) Sections incubated with α-zein antibody, followed by goat anti-rabbit/colloidal gold, and enhanced with silver intensification reagent. Staining deposits in the subaleurone layer (not visible at this magnification) gradually increase in diameter and intensity between SE-1 and SE-3. At SE-4, and deeper cell layers, the staining becomes more or less constant. **(Inset)** High magnification view of the fifth starchy endosperm layer. Solid circular deposits of silver occur over protein bodies (arrowheads).
(C) Sections incubated with β-zein antibody, followed by goat anti-rabbit/colloidal gold, and enhanced with silver intensification reagent. Staining patterns in the subaleurone and first starchy endosperm layer are solid circles (not visible at this magnification); protein bodies farther from this layer generally immunostain with open circular patterns. The labeling intensity is greatest in cell layers SE 2-4, and decreases in deeper layers of the endosperm. **(Inset)** High magnification view of the fifth starchy endosperm layer; β-zein is peripherally distributed in the protein bodies; some internal inclusions also immunostain (arrowhead).
(D) Sections incubated with γ-zein antibody, followed by goat anti-rabbit/colloidal gold, and enhanced with silver intensification reagent. The immunostaining patterns are as described for β-zein [**(C)**], but the staining intensity is lower. **(Inset)** High magnification view of the fifth starchy endosperm layer, demonstrating the peripheral distribution of γ-zein; some internal inclusions also immunostain (arrowhead). The staining intensity is generally lower than for the β-zein antibody [see **(C)**].
(E) Section immunostained with preimmune serum, followed by goat anti-rabbit/colloidal gold, and enhanced with silver intensification reagent. Little specific staining is observed in these sections; a slight darkening of the aleurone occurs in all sections, and is caused by the reaction of the silver-enhancement reagent with the lipid bodies. **(Inset)** High magnification view of the fifth starchy endosperm layer. Slight background labeling is seen, but no specific immunostaining is observed over protein bodies.

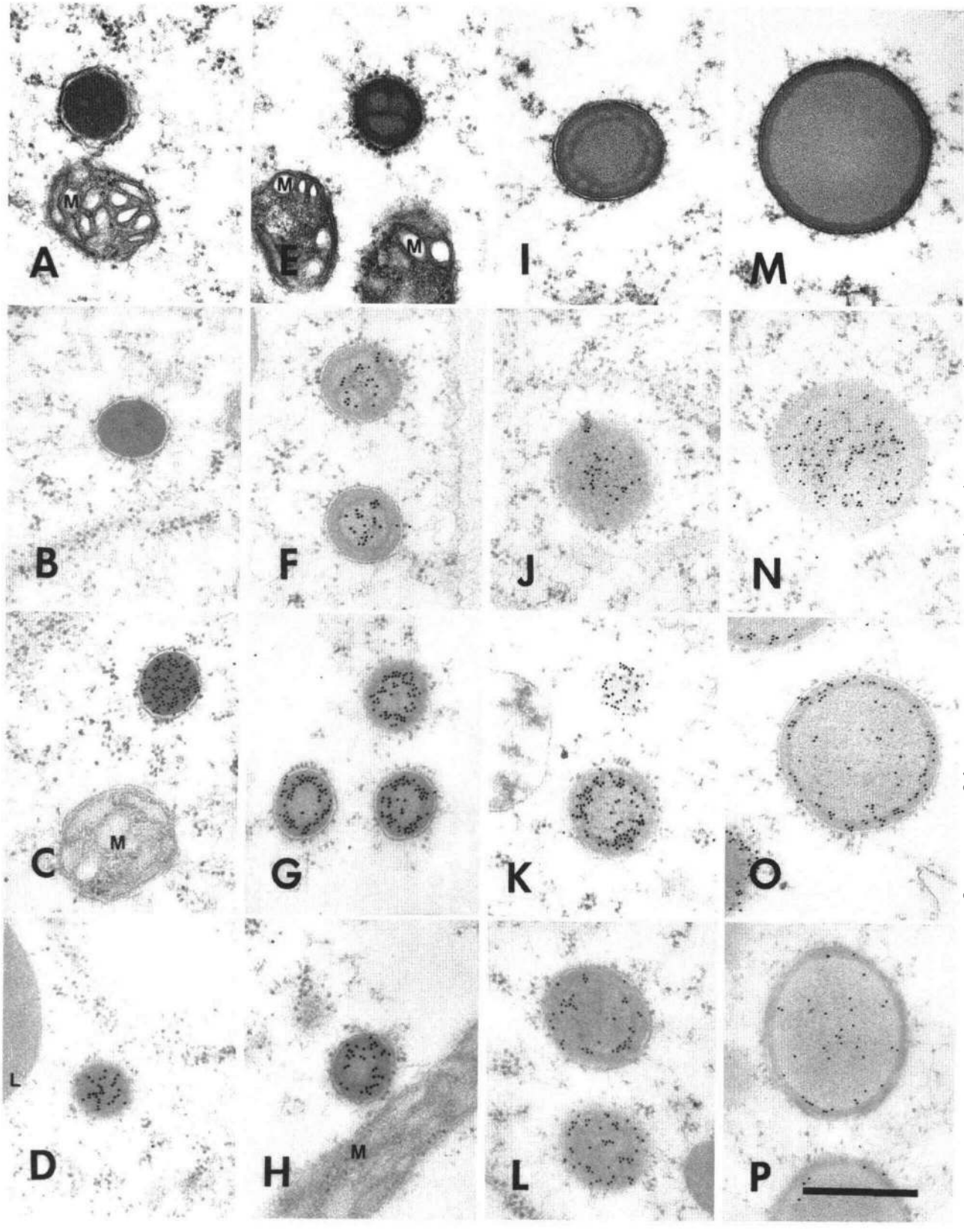

that of β-zein, the intensity of the immunostaining was lower for γ-zein (Figure 2D, inset).

Controls

Immunostaining with a concentration of preimmune serum similar to that used for the primary antiserum gave very low levels of nonspecific staining (Figure 2E). In all of the immunostained preparations, colloidal gold marker was predominantly limited to protein bodies; background labeling over the cytoplasm, other organelles, and cell walls was extremely low (Figures 2B to 2E).

The aleurone layer darkened when sections were reacted with the silver enhancement reagent, but this was easily differentiated from the immunostaining reaction (Figures 2B to 2E). The reaction with the aleurone layer arose from an interaction with the lipid bodies within these cells. The staining was proportional to the amount of lipid deposition, and was prevented by eliminating the osmium tetroxide post-fixation (not shown).

Electron Microscopy

A detailed study of maize endosperm ultrastructure was described previously (Khoo and Wolf, 1970). Therefore, in Figures 3 and 4, we present micrographs of medial sections that reflect only the distribution of zeins within protein bodies.

Because unequal cell divisions often occur, it is sometimes difficult to determine the exact position of a cell with respect to the aleurone layer. However, the protein bodies we describe are representative of those observed within a particular cell layer, with respect to both size and morphology. Also, the protein bodies within individual cells at both 14 DAP and 18 DAP were quite uniform in size and in the distribution of light- and dark-staining areas.

14 Days after Pollination

Subaleurone Layer. Protein bodies within this cell layer consisted primarily of dark-staining material; infrequently, small deposits of light-staining material were observed. The protein bodies in this cell layer were from 0.1 μm to 0.3 μm in diameter (Figures 3A to 3D).

A few protein bodies within the subaleurone layer were sparsely labeled with the α-zein antibody, but the vast majority of the protein bodies within this layer did not stain (Figure 3B). However, protein bodies within this layer were heavily and uniformly labeled by the β-zein antibody (Figure 3C). The immunolabeling of γ-zein (Figure 3D) in the subaleurone layer was similar to that of β-zein, although the reaction was not as intense as with the β-zein antibody.

First Starchy Endosperm Layer. Protein bodies in the first starchy endosperm layer ranged between 0.2 μm and 0.5 μm in diameter, and consisted mostly of dark-staining material with locules of light-staining material toward the interior regions (Figures 3E to 3H).

The locules of light-staining material were labeled with the α-zein antibody (Figure 3F). Both β- and γ-zein antibodies immunolabeled predominantly over the dark-staining regions of the protein bodies (Figures 3G and 3H, respectively). The labeling over the peripheral, dark-staining deposits often was preferentially distributed near the interface between the light- and dark-staining regions (Figure 3G). Immunostaining was also often observed over small, dark-staining deposits within the light-staining regions of protein bodies (Figures 3G and 3H); these deposits were often obscured by the gold particles. The immunostaining for γ-zein was not as uniform as that observed for β-zein.

Second Starchy Endosperm Layer. The protein bodies within the second starchy endosperm layer ranged from

Figure 3. Electron Micrographs Showing Representative Protein Bodies from Different Cell Layers of the Endosperm at 14 DAP.

The protein bodies are representative of the morphology and size of protein bodies within the cell layer indicated, and represent a developmental series (from left to right). In general, α-zeins are located in the light-staining regions, and β- and γ-zeins are located over the dark-staining regions. For immunostaining, sections were incubated in the indicated primary antibody and then in goat anti-rabbit/colloidal gold (10 nm). Bar = 0.5 μm. Abbreviations are as in Figure 1.

(A) to **(D)** Protein bodies from the subaleurone layer.

(A) Section stained with uranyl acetate and lead citrate.

(B) Section immunostained for α-zein.

(C) Section immunostained for β-zein.

(D) Section immunostained for γ-zein.

(E) to **(H)** Protein bodies from the first starchy endosperm layer. [Same sequence of stainings as in **(A)** to **(D)**.]

(G) The labeling for β-zein is preferentially distributed over the dark-staining region near the interface with the light-staining material.

(I) to **(L)** Protein bodies from the second starchy endosperm layer. [Same sequence of stainings as in **(A)** to **(D)**.]

(M) to **(P)** Protein bodies from the fifth starchy endosperm layer. [Same sequence of stainings as in **(A)** to **(D)**.]

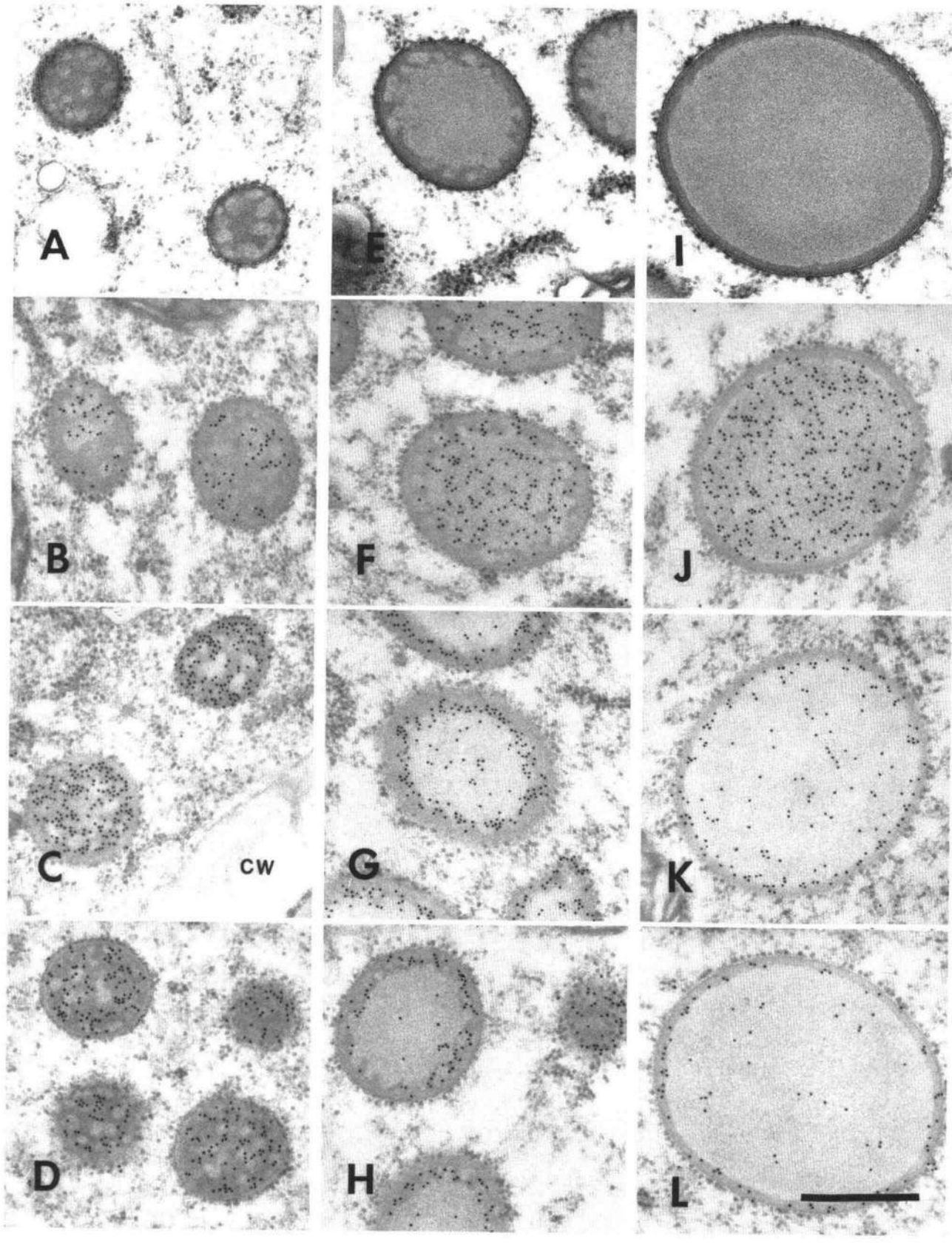

0.3 μm to 0.6 μm and consisted mostly of a central core of light-staining material surrounded by a peripheral ring of dark-staining material (Figures 3I to 3L). Small deposits of dark-staining material were frequently observed within the central region (not shown). Often, the interface between the light- and dark-staining regions was uneven, and small locules of light-staining material were frequently observed within the peripheral dark-staining regions.

Immunolabeling for α-zein was detected over the light-staining central regions of protein bodies within this cell layer (Figure 3J) and over the peripheral locules of light-staining material (not shown). Immunostaining for both β- and γ-zein occurred over the peripheral, dark-staining regions of protein bodies (Figures 3K and 3L, respectively). As with the immunostaining over protein bodies in the first starchy endosperm layer, γ-zein generally labeled less intensely than β-zein.

Third, Fourth, and Fifth Starchy Endosperm Layers. The diameter of protein bodies was found to increase progressively between the third and the fifth starchy endosperm layers; protein bodies in the fifth starchy endosperm layer were 0.6 μm to 0.9 μm in diameter (Figures 3M to 3P). The majority of protein bodies had a uniform, peripheral region of dark-staining material that surrounded an inner region of light-staining material. Small amounts of the dark-staining material were sometimes observed within the light-staining regions (not shown). These protein bodies were characteristic of those observed in cell layers farther from the aleurone layer, although the width of the peripheral dark-staining regions decreased slightly at greater distances from the aleurone layer (not shown).

The interior regions of protein bodies in the third starchy endosperm layer and those farther into the endosperm immunostained for α-zein (Figure 3N). Immunostaining patterns for β- and γ-zein (Figures 3O and 3P, respectively) were similar to those observed in protein bodies of the second starchy endosperm layer, although the density of labeling was lower.

18 Days after Pollination

Subaleurone Layer. The protein bodies in the subaleurone layer at 18 DAP were 0.3 μm to 0.6 μm in diameter and consisted of dark-staining material that surrounded interior locules of light-staining material (Figures 4A to 4D). Small amounts of the dark-staining material were sometimes observed within the light-staining regions (not shown). However, unlike the tissue sampled at 14 DAP, we observed no protein bodies that consisted only of dark-staining regions.

Immunogold labeling for α-zein was restricted to light-staining regions of the protein bodies (Figure 4B), whereas labeling for β- and γ-zein was restricted primarily to dark-staining regions (Figures 4C and 4D, respectively).

First Starchy Endosperm Layer. Protein bodies in the first starchy endosperm layer were 0.5 μm to 0.9 μm in diameter. The central region of these protein bodies consisted of light-staining material (Figures 4E to 4H); this region was sometimes interspersed with dark-staining material. The peripheral region of these protein bodies consisted primarily of dark-staining material, often with scalloped edges at the interface of the light- and dark-staining regions. Additionally, small locules of light-staining material were sometimes observed within the peripheral dark-staining regions (Figure 4E), often continuous with the central region.

Immunogold labeling for α-zein occurred predominantly over the light-staining regions of the protein bodies (Figure 4F), whereas labeling for β- and γ-zein was restricted primarily to dark-staining regions (Figures 4G and 4H, respectively). Most of the gold label was over the inner portion of the peripheral, dark-staining region, near the interface with the central light-staining areas (Figures 4G and 4H).

Second, Third, Fourth, and Fifth Starchy Endosperm Layers. Most of the protein bodies in these layers had a

Figure 4. Electron Micrographs Showing Representative Protein Bodies from Different Cell Layers of the Endosperm at 18 DAP.

Micrographs are representative of the morphology and size within the cell layer indicated. In general, α-zeins are located in the light-staining regions, and β- and γ-zeins are located over the dark-staining regions. For immunostaining, sections were incubated in the indicated primary antibody and then in goat anti-rabbit/colloidal gold (10 nm). Bar = 0.5 μm. Abbreviations are as in Figure 1.

(A) to **(D)** Protein bodies from the subaleurone layer.

(A) Section stained with uranyl acetate and lead citrate.

(B) Section immunostained for α-zein.

(C) Section immunostained for β-zein.

(D) Section immunostained for γ-zein.

(E) to **(H)** Protein bodies from the first starchy endosperm layer. [Same sequence of stainings as in **(A)** to **(D)**.]

(G) The labeling for β-zein is preferentially distributed over the dark-staining region near the interface with the light-staining material.

(I) to **(L)** Protein bodies from the fifth starchy endosperm layer. [Same sequence of stainings as in **(A)** to **(D)**.]

(L) The labeling for γ-zein is preferentially distributed over the dark-staining region near the interface with the light-staining material.

uniform region of dark-staining material that surrounded an inner region of light-staining material (Figures 4I to 4L). Small amounts of the dark-staining material were sometimes observed within the light-staining regions, as were central inclusions of dark-staining material (not shown). The diameter of protein bodies was found to increase progressively between the second and the fifth starchy endosperm layers; protein bodies in the fifth starchy endosperm layer were 0.8 μm to 1.4 μm in diameter. These protein bodies were characteristic of those observed in cell layers farther from the aleurone layer, although the width of the peripheral dark-staining regions decreased slightly in cells deeper in the endosperm (not shown).

Immunogold labeling for α-zein occurred predominantly over the light-staining regions of the protein bodies (Figure 4J). The β- and γ-zein immunolabeling occurred over the dark-staining regions of these protein bodies (Figures 4K and 4L, respectively). Most of the gold label for β- and γ-zein was over the inner portion of the peripheral, dark-staining region, near the interface with the central light-staining areas (Figure 4L). Some internal labeling for β- and γ-zein was observed over the light-staining interior regions, but this often correlated with internal deposits of dark-staining material. As with the immunostainings at 14 DAP, the γ-zein immunoreaction was less intense than that observed for β-zein.

Controls

In all of the immunostained preparations, colloidal gold marker was predominantly limited to protein bodies; background labeling over the cytoplasm, other organelles, and cell walls was extremely low (Figures 3 and 4). Substitution of preimmune serum resulted in negligible background, similar to that previously demonstrated (Lending et al., 1988).

DISCUSSION

The in situ immunocytochemical localizations presented here reveal distinct patterns of zein deposition within protein bodies as they form within the rough endoplasmic reticulum. We previously showed that protein bodies isolated from developing endosperm vary in size, and that there are different patterns of zein distribution (Lending et al., 1988; Larkins et al., 1989). Our current observations demonstrate that the variation in size and zein composition is dependent on the position of a protein body within the endosperm. The outer cell layers of the endosperm have a higher concentration of β- and γ-zeins; protein bodies within these cells are smaller and contain less α-zein than those in internal regions of the endosperm.

The differences in size and zein composition of protein bodies in developing endosperm correlated with the stages of cell maturity. The pattern of development within corn endosperm has been previously established, and the subaleurone cells are considered to be meristematic; thus, these cells function like a cambial layer (Fisk, 1927; Randolph, 1936). Mitosis in the endosperm becomes limited to the region directly beneath the aleurone layer by 10 DAP; few mitotic cells are observed in the interior of the endosperm (Kiesselbach, 1949). We consistently observed a gradient in protein body size and zein content throughout development. As cells matured, the size of protein bodies increased, concomitant with an increase in the amount of α-zein. Also, as the seed matured, larger protein bodies were observed progressively closer to the aleurone layer. Thus, even though we observed static images, the gradient of protein body size from the subaleurone region to the interior of the endosperm reflects the pattern of cell maturation.

Based on our examination of the distribution of the various zeins in protein bodies within adjacent cells at 14 DAP, we can propose a descriptive model for the pattern of zein deposition during protein body formation, as shown in Figure 5. Initial accretions within the rough endoplasmic reticulum consist of dark-staining deposits of both β- and γ-zeins, which contain little or no α-zein (Figure 5A). Subsequently, α-zein begins to accumulate and is observed as discrete, light-staining locules within the β- and γ-zeins (Figure 5B). As the interior of the protein body fills with α-zein, the locules of α-zein fuse and aggregate to form a central core; some smaller locules of α-zein remain and are interspersed in the outer region of the protein body (Figure 5C). The dark-staining region that contains β- and γ-zein forms a continuous layer around the periphery of the protein body; the interface with α-zein is typically scalloped and uneven at this stage, a reflection of the coalescing locules of α-zein. In the final stages of protein body maturation, α-zein fills most of the core of the protein body and is surrounded by a thin layer of β- and γ-zeins (Figure 5D). Small, dark-staining patches of β-zein and, more commonly, γ-zein may occur within the interior region.

Although this model is based on the examination of many immunostainings, some structural features of protein bodies are not explained. First, the inclusions of β- and γ-zein that occur within the interior regions (that consist mostly of α-zein) may form strands that run throughout the protein body, or they may form small aggregates within the α-zein. Resolution of this question will require immunostainings of serial sections through protein bodies. Second, the β- and γ-zeins are not uniformly distributed throughout the dark-staining material; they are predominantly located near the interface of light- and dark-staining regions (Figures 3G and 3L; Figures 4G to 4L). In fact, little immunostaining was observed with any of the antibodies on the outermost portions of the peripheral, dark-staining regions. It may be possible to resolve more clearly the location of

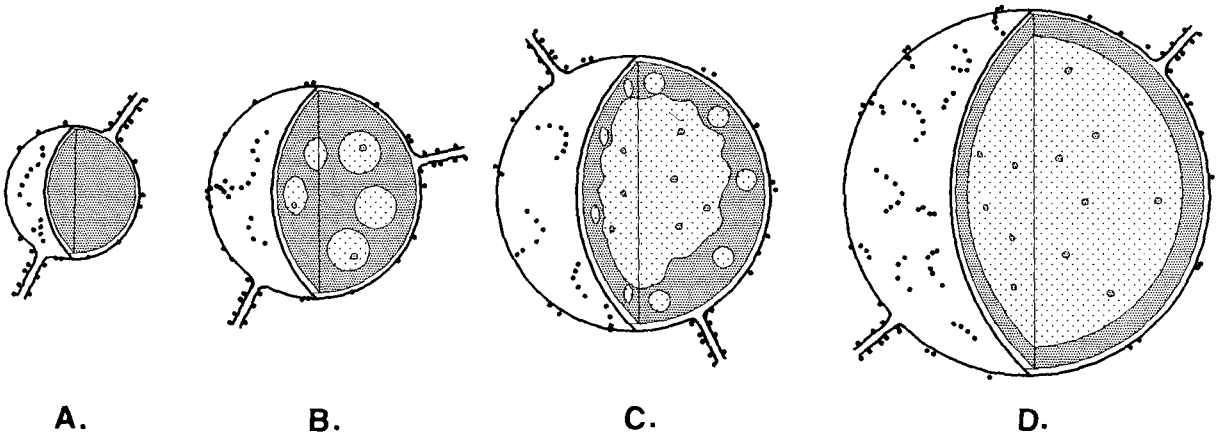

Figure 5. Development of Protein Bodies in Maize Endosperm (Not to Scale).

The heavily stippled regions correspond to regions that are rich in β- and γ-zeins, and the lightly stippled regions correspond to regions rich in α-zein. The protein body is surrounded by rough endoplasmic reticulum (dark dots represent ribosomes). Some β- and γ-zeins are found within the regions that consist primarily of α-zein (heavily stippled inclusions); we do not know whether these are strands of protein that run through the protein body, or small, individual aggregates. See Discussion for details.

the proteins by immunolabeling the various zein classes with smaller sized (3-nm) colloidal gold conjugates to increase the labeling density. More dense immunolabeling of α-zein was detected when 3-nm goat anti-rabbit/colloidal gold conjugates were used (C.R. Lending and B.A. Larkins, unpublished observations). However, the gold labeling was more difficult to observe at the magnification used to illustrate the present study. Some of the regions that are not heavily labeled may contain δ-zein; we are currently obtaining antibodies to δ-zein to determine its location within protein bodies.

It is not clear from our studies whether or not specific interactions occur between the different structural classes of zeins. The mechanism by which the α-zeins pass through the β- and γ-zeins is unknown. Since the β- and γ-zeins are highly cross-linked by disulfide bonds, it would appear that some of these bonds may be reduced as the protein body increases in size. Alternatively, cross-linkage of disulfides may not occur during the initial stages of protein body formation, but only after the protein body has matured.

At 18 DAP, the zein distribution within protein bodies in cells of the second starchy endosperm layer was similar to that in cells deeper in the endosperm; a central region that contained α-zein was surrounded by a peripheral layer of β- and γ-zeins. This morphology was similar to the protein bodies in endosperm at 14 DAP in the third starchy endosperm layer and in cell layers progressively farther from the aleurone, although protein bodies from endosperm at 18 DAP were larger than those at 14 DAP. Although protein bodies within the subaleurone layer and the first layers of the starchy endosperm at 18 DAP continued to increase in size, they eventually contained a higher proportion of β- and γ-zein compared with α-zein than the proportions that were observed in cells farther from the aleurone layer (not shown). The increased levels of β- and γ-zein proteins in the protein bodies of the cell layers closest to the aleurone layer may reflect higher proportions of both β- and γ-zein mRNAs than of α-zein mRNAs.

All of the previous studies on developing endosperm were carried out prior to the availability of the current embedding resins (e.g., LR White) and the routine application of immunocytochemical techniques for protein localization. We found that LR White resin maintained excellent antigenicity for the zeins and enabled us readily to infiltrate thick tissue pieces that contained considerable starch deposits. It was easy to obtain semi-thin (0.75 μm) sections for light microscopy, thus facilitating high-resolution studies by electron microscopy. The use of immunocytochemical procedures for both the light and electron microscopy provided complementary information, at different levels of resolution, about the distribution of the various zeins.

We do not yet know whether the proposed model is applicable to other members of the *Panicoideae*, but light- and dark-staining regions can also be seen in protein bodies in developing sorghum (Taylor, Schüssler, and Liebenberg, 1984, 1985). We are currently investigating the interactions of the different classes of zeins through the study of several maize mutant lines that alter protein body composition.

METHODS

Chemicals and Plant Material

Bovine serum albumin (BSA), Tris base, Tween 20, and goat anti-rabbit immunoglobulin G (IgG) were from Sigma (St. Louis, MO). LR White resin was from Structure Probe, West Chester, PA. All other chemicals were reagent grade.

Maize plants (*Zea mays*) of the inbred line W64A were grown at the Purdue University Agronomy Farm, West Lafayette, IN, during the summers of 1987 and 1988.

Fixation and Embedment of Seeds

Maize seeds were prepared for light and electron microscopy and immunocytochemistry by fixation in a solution that contained 1% (v/v) glutaraldehyde and 4% (w/v) freshly prepared formaldehyde in phosphate buffer (50 mM KH_2PO_4/K_2HPO_4, pH 7.0). Seeds at either 14 DAP or 18 DAP were dissected from cobs, immersed in ice-cold fixative, and sliced into 2-mm-thick longitudinal sections; the fixed material was then stored at 4°C until it was processed further.

Samples were brought to room temperature and processed; all steps prior to polymerization of the plastic were performed at room temperature. The fixed seeds were further dissected, and portions from the side of the seed were removed and processed for microscopy and immunocytochemical stainings. Tissue slices were washed three times (5 min each) with phosphate buffer and post-fixed for 2 hr in 2% (w/v) osmium tetroxide in phosphate buffer. Samples were washed three times with phosphate buffer, two times with distilled water (5 min each), and then dehydrated in a graded ethanol series: 10 min each in 10%, 30%, 50%, 70%, 90%, and 100% ethanol. After an additional 10 min in fresh 100% ethanol, the samples were infiltrated with 30% LR White resin in ethanol for 1 hr, 60% LR White resin in ethanol for 1 hr, and then placed in 100% LR White resin overnight. The resin was replaced with fresh resin the following morning. The samples were infiltrated for an additional 5 hr and then polymerized in Beem capsules or aluminum embedding molds at 55°C in a sealed oven purged with nitrogen. After 24 hr, samples were removed from the molds.

For light microscopy, semi-thin sections (0.75 μm) were cut with glass knives on a Sorvall MT-2B ultramicrotome (E.I. DuPont, Wilmington, DE); all sections were cut perpendicular to the aleurone layer so that the pericarp, aleurone, and 10 to 20 cell layers of the endosperm were included. Several sections were collected onto glass slides coated with 1% (w/v) gelatin, and the slides were dried at 60°C on a hot plate; these slides were used for immunostaining as described below. For conventional light microscopy, sections were collected onto uncoated glass slides and stained for 30 sec with 0.05% basic fuchsin in 5% (v/v) ethanol and 25 mM KH_2PO_4/Na_2HPO_4, pH 7.0. Slides were examined with a Vanox AH-2 photomicroscope (Olympus Optical, Tokyo, Japan), and photographs were recorded on Kodak 2415 Technical Pan Film (Eastman Kodak, Rochester, NY).

For electron microscopy, tissue samples that had been examined by light microscopy were trimmed to include a portion of the pericarp, the aleurone layer, and 5 to 15 cell layers of the endosperm. Sections were cut with a diamond knife on an Ultracut E ultramicrotome (Reichert-Jung, Vienna, Austria) and collected on copper grids coated with Formvar and carbon for immunocytochemical staining as described below. Some sections were not immunostained but were post-stained with uranyl acetate for 5 min and lead citrate for 10 min. Grids were examined with a Philips EM-400 electron microscope (Philips Electronic Instruments, Mahwah, NJ).

Purification of Zein Proteins and Preparation of Antisera

Zeins were purified, and antibodies specific for α-, β-, and γ-zein were prepared and characterized as described previously (Lending et al., 1988). Crude antisera were used in all immunostaining procedures.

Preparation of Colloidal Gold Conjugate

Goat anti-rabbit/colloidal gold conjugates for immunocytochemical stainings were prepared by a method similar to that of Slot and Geuze (1985) as described by Lending et al. (1989). Immunoaffinity-purified goat anti-rabbit IgG was complexed to colloidal gold with a mean diameter of 10 nm. The conjugates were separated from unbound antibodies by centrifugation in a 10% to 30% linear glycerol gradient that contained 20 mM Tris-HCl, 150 mM NaCl, 1% (w/v) BSA, and 20 mM sodium azide (Slot and Geuze, 1981). The gold conjugates were stored at 4°C and were diluted to a pale pink color immediately before use.

Immunocytochemical Staining—Light Microscopy

Semi-thin sections were stained by a technique modified from VandenBosch (1986). Sections on the slides were encircled by a thin line of nail polish to minimize the amount of reagents needed for the immunostaining. The sections were incubated for 10 min with TBS-T-B [20 mM Tris-HCl, pH 8.2, containing 500 mM NaCl, 0.3% (v/v) Tween 20, and 1% (w/v) BSA]. All incubations were carried out in a covered Petri plate lined with wetted paper to minimize evaporation; all steps were carried out at room temperature. The TBS-T-B was removed, and the sections were incubated for 2 hr with the primary antibody diluted in TBS-T-B. Anti-α-, anti-β-, and anti-γ-zein were used at dilutions of 1:2000, 1:1000, and 1:500, respectively. Slides were washed by immersion in stirred TBS-T [20 mM Tris-HCl, pH 8.2, containing 500 mM NaCl and 0.3% (v/v) Tween 20] in a staining jar, 3 × 20 min each. Sections were covered with goat anti-rabbit/colloidal gold diluted to a pale pink color in TBS-T-B and incubated for 1 hr. Slides were washed by immersion in stirred TBS-T in a staining jar, 3 × 20 min each, and then for 10 min in distilled water. Slides were blotted to remove excess moisture, and silver enhancement of the colloidal gold was done for 10 min with Intense II (Janssen Life Sciences Products, Olen, Belgium) according to the manufacturer's instructions. The primary antibody was substituted with a similar dilution of preimmune serum for immunocytochemical controls.

Immunocytochemical Staining—Electron Microscopy

Thin sections were immunostained essentially as described by Lending et al. (1988). Primary antibody concentrations were 1:2000, 1:1000, and 1:500 for α-, β-, and γ-zein antibodies,

respectively. Instead of washing the grids by immersion in stirred TBS-T, the grids were incubated in 200-μL drops of TBS-T, 3 × 15 min each. Sections were post-stained for 5 min in 2.5% (w/v) aqueous uranyl acetate, rinsed, and then post-stained in Reynold's lead citrate for 2 min; the brief lead citrate post-staining enhanced the contrast of the sections to allow better discrimination of the light- and dark-staining regions of protein bodies than was possible when uranyl acetate alone was used. The grids were then rinsed three times with distilled water, blotted dry, and examined. The primary antibody was substituted with a similar dilution of preimmune serum for immunocytochemical controls.

ACKNOWLEDGMENTS

This research was supported by National Institutes of Health grant GM36790 (to B.A.L.) and by a grant from Lubrizol Genetics, Madison, WI. This is Journal Paper No. 12175 from the Purdue University Agricultural Experiment Station. We acknowledge the Electron Microscopy Center in Agriculture at Purdue University for the use of its facilities, and thank Charles Bracker for his helpful discussions. We thank Katy L. Shaw and Lynette Vos for their excellent technical assistance, and Virginia Russell, Mark Shotwell, and John Wallace for useful discussions.

Received September 7, 1989.

REFERENCES

Dierks-Ventling, C., and Ventling, D. (1982). Tissue-specific immunofluorescent localization of zein and globulin in *Zea mays* (L) seeds. FEBS Lett. **144,** 167–172.

Esen, A. (1986). Separation of alcohol-soluble proteins (zeins) from maize into three fractions by differential solubility. Plant Physiol. **80,** 623–627.

Felker, F.C. (1987). Ultrastructure of maize endosperm suspension cultures. Am. J. Bot. **74,** 1912–1920.

Fisk, E.L. (1927). The chromosomes of *Zea mays*. Am. J. Bot. **14,** 53–75.

Khoo, U., and Wolf, M.J. (1970). Origin and development of protein granules in maize endosperm. Am. J. Bot. **57,** 1042–1050.

Kiesselbach, T.A. (1949). The structure and reproduction of corn. University of Nebraska Agricultural Experiment Station. Res. Bull. **161,** 1–96.

Kirihara, J.A., Hunsperger, J.P., Mahoney, W.C., and Messing, J.W. (1988). Differential expression of a gene for a methionine-rich storage protein in maize. Mol. Gen. Genet. **211,** 477–484.

Kyle, D., and Styles, E.D. (1977). Development of aleurone and sub-aleurone layers in maize. Planta **137,** 185–193.

Landry, J., and Moureaux, M.T. (1970). Heterogeneite des glutelines du grain de mais: Extraction selective et composition en acides amines des trois fractions isolees. Bull Soc. Chem. Biol. **52,** 1021–1037.

Larkins, B.A., and Hurkman, W.J. (1978). Synthesis and deposition of zein in protein bodies of maize endosperm. Plant Physiol. **62,** 256–263.

Larkins, B.A., Pedersen, K., Marks, M.D., and Wilson, D.R. (1984). The zein proteins of maize endosperm. Trends Biochem. Sci. **9,** 306–308.

Larkins, B.A., Lending, C.R., Wallace, J.C., Galili, G., Kawata, E.E., Geetha, K.B., Kriz, A.L., Martin, D.N., and Bracker, C.E. (1989). Zein gene expression during maize endosperm development. In The Molecular Basis of Plant Development, R.B. Goldberg, ed (New York: Alan R. Liss, Inc.), pp. 109–120.

Lee, K.H., Jones, R.A., Dalby, A., and Tsai, C.Y. (1976). Genetic regulation of storage protein content in maize endosperm. Biochem. Genet. **14,** 641–650.

Lending, C.R., Kriz, A.L., Larkins, B.A., and Bracker, C.E. (1988). Structure of maize protein bodies and immunocytochemical localization of zeins. Protoplasma **143,** 51–62.

Lending, C.R., Chesnut, R.S., Shaw, K.L., and Larkins, B.A. (1989). Immunolocalization of avenin and globulin storage proteins in developing endosperm of *Avena sativa* L. Planta **178,** 315–324.

Ludevid, M.D., Torrent, M., Martinez-Izquierdo, J.A., Puigdomènech, P., and Palau, J. (1984). Subcellular localization of glutelin-2 in maize (*Zea mays* L.) endosperm. Plant Mol. Biol. **3,** 227–234.

Prat, S., Pérez-Grau, L., and Puigdomènech, P. (1987). Multiple variability in the sequence of a family of maize endosperm proteins. Gene **52,** 41–49.

Randolph, L.F. (1936). Developmental morphology of the caryopsis in maize. J. Agric. Res. **53,** 881–916.

Schel, J.H.N., Kieft, H., and VanLammeren, A.A.M. (1984). Interactions between embryo and endosperm during early developmental stages of maize caryopses (*Zea mays*). Can. J. Bot. **62,** 2842–2853.

Slot, J.W., and Geuze, H.J. (1981). Sizing of protein A-colloidal gold probes for immunoelectron microscopy. J. Cell Biol. **90,** 533–536.

Slot, J.W., and Geuze, H.J. (1985). A new method of preparing gold probes for multiple labeling cytochemistry. Eur. J. Cell Biol. **38,** 87–93.

Taylor, J.R.N., Schüssler, L., and Liebenberg, N.v.d.W. (1984). Location of zein-2 and crosslinked kafirin in maize and sorghum protein bodies. J. Cereal Sci. **2,** 249–255.

Taylor, J.R.N., Schüssler, L., and Liebenberg, N.v.d.W. (1985). Protein body formation in starchy endosperm of developing *Sorghum bicolor* (L.) Moench seeds. S. Afr. J. Bot. **51,** 35–40.

VandenBosch, K.A. (1986). Light and electron microscopic visualization of uricase by immunogold labelling of sections of resin-embedded soybean nodules. J. Microscopy **143,** 187–197.

Wallace, J.C., Lopes, M.A., Paiva, E., and Larkins, B.A. (1989). New methods for extraction and quantitation of zeins reveal a high content of gamma-zein in modified opaque-2 maize. Plant Physiol., in press.

Wolf, M.J., Khoo, U., and Seckinger, H.L. (1969). Distribution and subcellular structure of endosperm protein in varieties of ordinary and high-lysine maize. Cereal Chem. **46,** 253–263.